GSC Advanced Research and Reviews

eISSN: 2582-4597 CODEN (USA): GARRC2

Cross Ref DOI: 10.30574/gscarr

Journal homepage: https://gsconlinepress.com/journals/gscarr/

(Research Article)

Simulation of the operation of a prototype of indirect solar dryer for drying cassava

Guy Clarence SEMASSOU [1, *], Alain TOSSA [2], Roger Houêchéné AHOUANSOU [2] and Neal ADJOVI [2]

[1] Laboratory of Energetics and Applied Mechanics (LEMA), University of Abomey-Calavi, 01 BP 2009 Cotonou, Benin.
[2] Department of Mechanical and Energy Engineering, University of Abomey-calavi, (Abomey-calavi), Benin.

GSC Advanced Research and Reviews, 2022, 12(03), 051–063

Publication history: Received on 29 July 2022; revised on 30 August 2022; accepted on 01 September 2022

Article DOI: https://doi.org/10.30574/gscarr.2022.12.3.0231

Abstract

This work consisted in the simulation of the operation of a prototype of a large capacity indirect solar dryer intended to dry 501.4 kg of fresh cassava pieces per drying cycle. It is designed to lower the water content of cassava pieces from 62% to 17% on a wet basis under optimal drying conditions, in order to improve the quality of products from the dried cassava pieces and to meet the standards of the international market. The modeling of the physical phenomena at the level of the dryer was done to follow the evolution of the various parameters influencing the drying. These phenomena were translated by a system of equations in order to simulate the operation of the dryer. Solving all of these equations allowed us to determine the temperature evolution of the different elements of the solar dryer and then to determine the drying kinetics of the cassava pieces. The use of this dryer will not only take advantage of the available solar energy but also guarantee the nutritional value of products derived from cassava pieces.

Keywords: Simulation; Solar dryer; Cassava pieces; Water content; Drying kinetic

1. Introduction

Agriculture is the main economic sector for many African states in general [1]. It represents, according to World Bank statistics, 17% of the GDP of the entire continent and about 30% of the GDP of all the countries of Sub-Saharan Africa excluding South Africa. [1]. In Benin in particular, the contribution of agriculture to the economy remains fundamental since the latter employs 70% of the active population and contributes 40% to the GDP in 2009 [2]. It is therefore clear that agriculture is the main sector on which the survival of the majority of the African population depends. In developing countries, agricultural production is often characterized by temporary harvest surpluses that current conservation methods cannot control. Each year, producers record huge post-harvest losses that range between 10 and 60% of production, depending on the products and production areas [3]. Faced with this situation, agricultural productivity surpluses require the development of appropriate conservation techniques in order to reduce post-harvest losses and ensure the permanent availability of agricultural products on local, regional and international markets. In developing countries, the simplest and oldest method of drying is traditional drying. This type of drying consists of exposing agricultural products directly to the sun without special equipment. The main purpose of this drying method is to extract a large part of the water contained in the product in order to greatly reduce the various reactions involved in the decomposition of the product. This practice, which seems satisfactory for many African producers, unfortunately exposes the products to various contaminations, to biological and microbiological degradation (rapid destruction of vitamins A and C, by exposure to the sun), and to photooxidation [4].

Nowadays, several powerful technologies of electric dryers are put on the market [5]. However, one of the main constraints is related to the fact that producers cannot easily access the electricity essential to the operation of these dryers. In addition, several agricultural solar dryers are designed in Benin and in the sub-region, but generally, there

* Corresponding author: Guy Clarence SEMASSOU
Department of Mechanical and Energy Engineering, University of Abomey-calavi, (Abomey-calavi), Benin.

are no large capacity agricultural solar dryers intended for cassava drying. The seashell solar dryer, tested for the first time in Senegal and widely used in Burkina Faso, is a reliable, resistant dryer that requires very little maintenance but does not allow the various drying parameters to be controlled [6]. The cabinet-type indirect solar dryer [7], made in Algeria and intended for drying apricots, is a dryer that has the advantage of protecting the product against bad weather and ultraviolet radiation, but it has a capacity limited to 25 kg. At the School of Energy and Environmental Studies in India, Dilip R. et al. [8] used in their work, an indirect solar dryer with forced convection composed of a solar thermal collector and a drying chamber. This dryer makes it possible to reach drying temperatures sufficient for drying several products (fruits and vegetables) but does not make it possible to effectively control the speed of air flow over the products. Dilip J. [9] has developed a new type of natural convection dryer with a thermal storage unit. This dryer is intended for drying onions with an estimated drying capacity of 90 kg and allows faster drying than traditional dryers but does not allow the speed of air flow on the products to be controlled. Singh S et al. [10], carried out an experimental study with a solar dryer of simple greenhouse design. This type of dryer makes it possible to dry the products quickly but does not make it possible to control the temperature and the speed of drying.

2. Material and methods

2.1. Materials

The prototype solar dryer studied is of the indirect type with forced convection; it is composed of two parts:

- A South-East oriented hot air production unit (solar thermal air collector, one of which is inclined at 20° and the other inclined at 55°);
- A drying chamber (L = 5 m, W = 5 m, H = 3.5 m) equipped with 140 drying racks measuring 0.6 m x 0.6 m.

Figure 1 shows an isometric view of the dryer prototype, Figure 2 shows the North-West facade with the aerodynamic flows inside the dryer, Figure 3 shows the North-West facade and Figure 4 shows the South-West facade. West of the dryer prototype. These figures are made with SOLIDWORKS 2017 software.

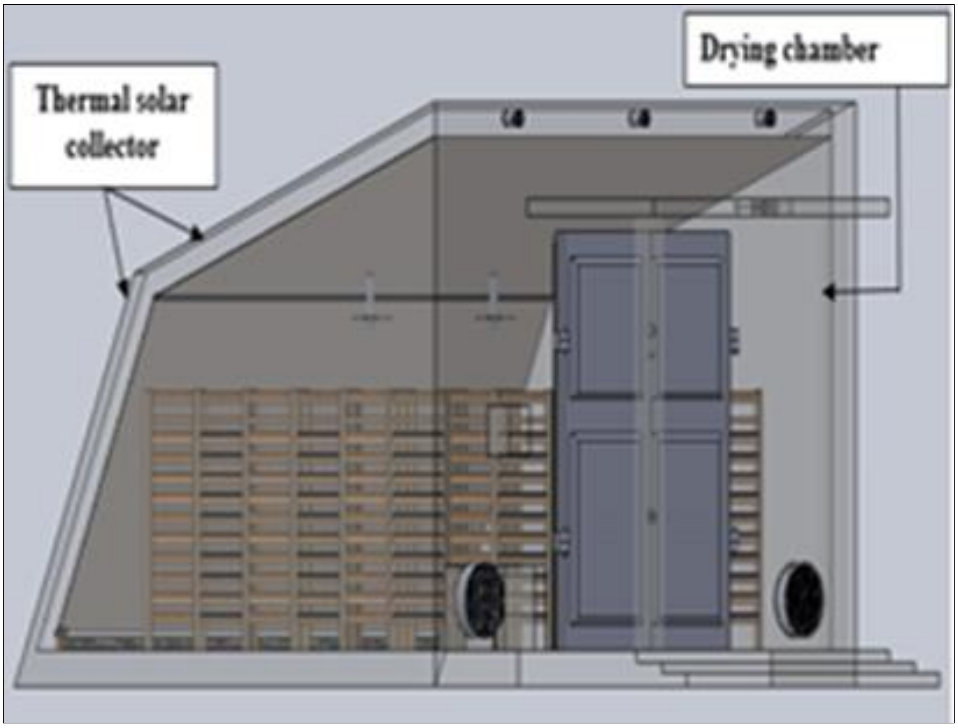

Figure 1 Isometric view of indirect solar dryer

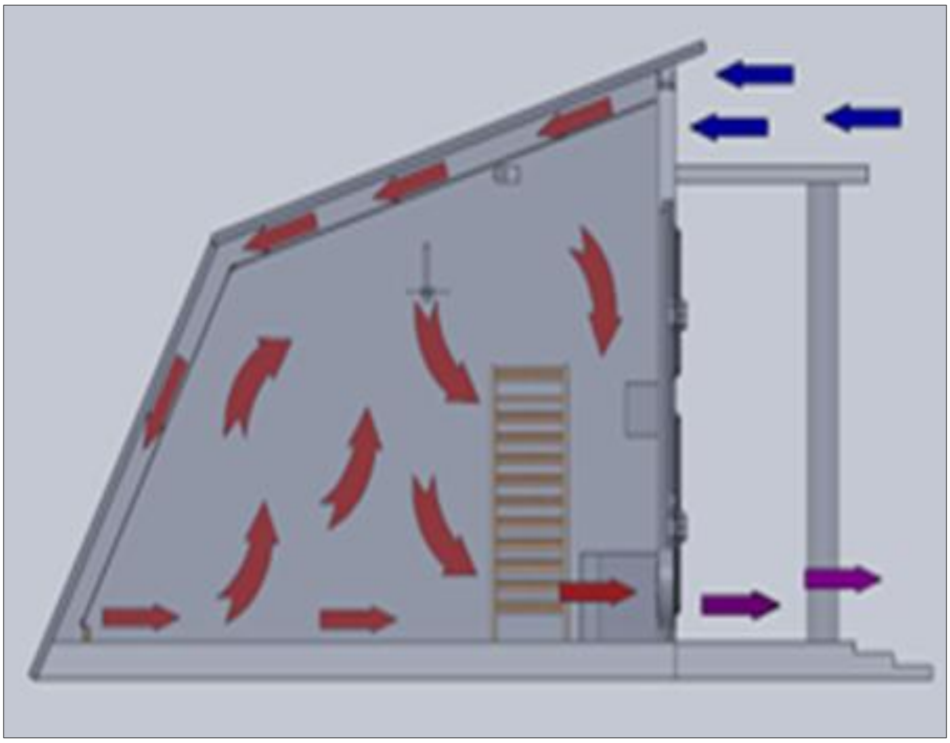

Figure 2 Presentation of the North-West facade with the direction of the air flows

Figure 3 Presentation of the North-West facade

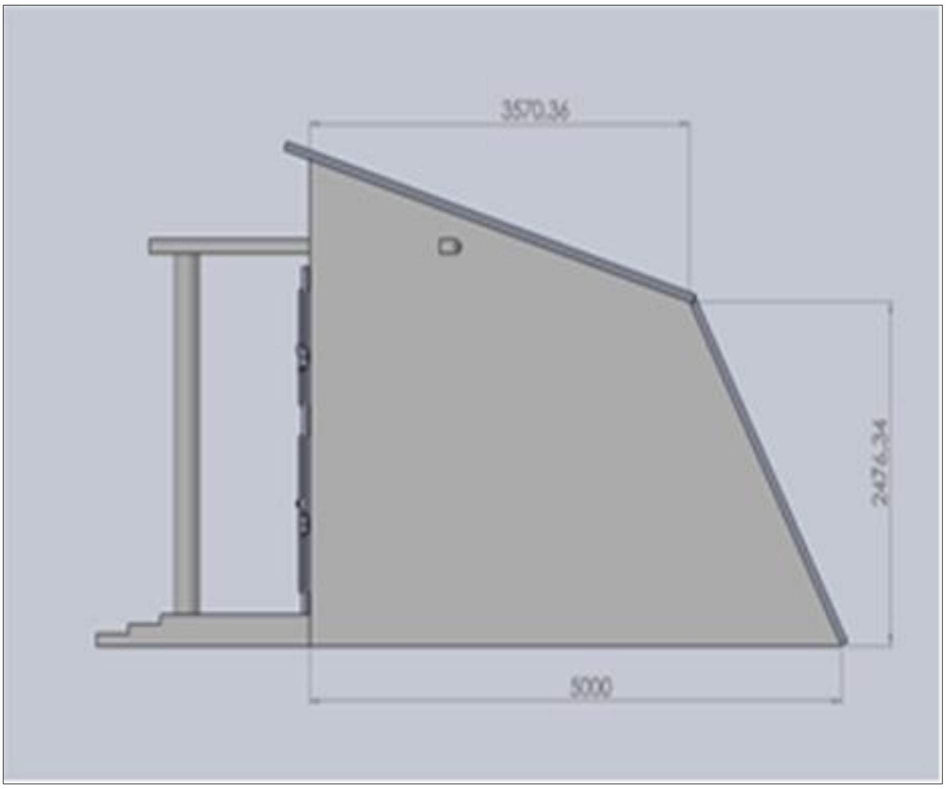

Figure 4 Presentation of South-West facade

2.2. Methods

To simulate the operation of the entire indirect solar dryer, we have developed a numerical model based on the global balance method (heat and mass balance). The Page model is the model used to simulate the evolution of the water content of cassava pieces as a function of time.

The establishment of the numerical model is based on the following simplifying assumptions:

- The temperatures of the absorbers are assumed to be uniform over their entire surface;
- The ground temperature is taken equal to the indoor air temperature;
- The air temperature inside the dryer is uniform at all times;
- In each part of the system, the flow is unidirectional;
- The spreading of cassava pieces on the racks is assumed to be homogeneous;
- No chemical reaction takes place in the product;
- The temperature and water content are uniform inside the product;
- One neglects the deformation of the product during the drying.

The different transfer modes that govern the operation of the thermal solar collector and that of the drying chamber are illustrated in Figures 5 and 6 in order to predict the thermal behavior of the dryer and the drying kinetics of the cassava pieces. The balance equations are established for absorber 1, absorber 2, the aluminum plate, the heat transfer fluid (the air leaving the thermal solar collector), the vertical walls of the drying chamber and the product.

2.2.1. Modeling of the thermal solar collector

The different exchanges that take place at the level of the collector are summarized in figure 5.

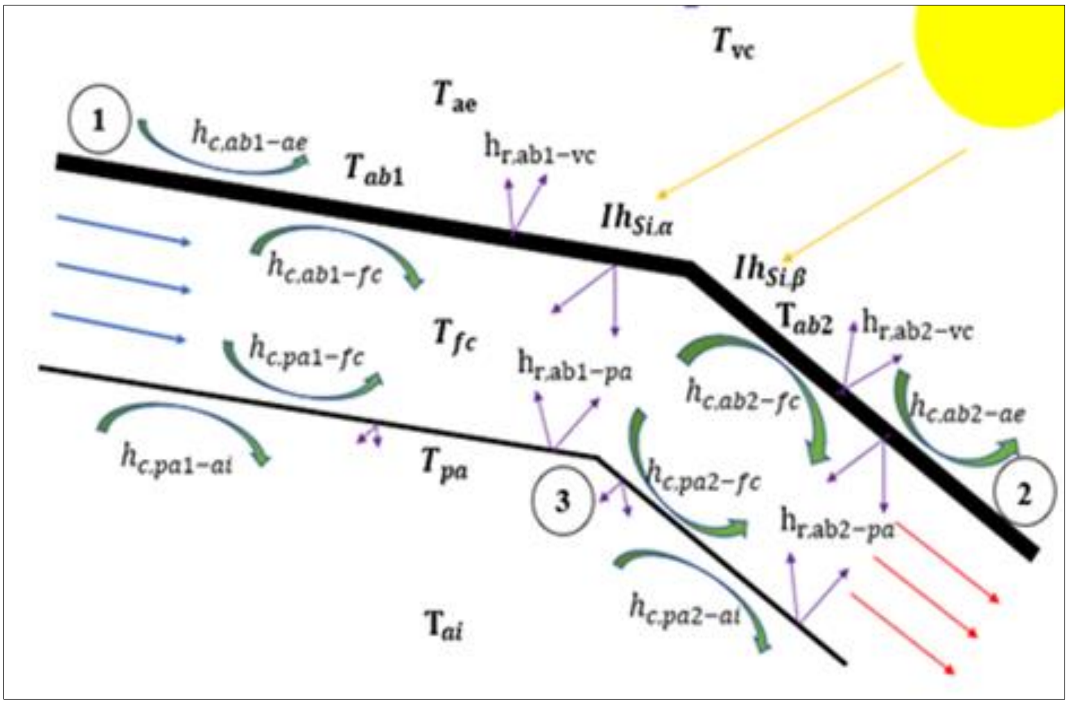

1: Absorber 1: 2: Absorber 2; 3: Aluminum plate

Figure 5 Schematic representation oh heat exchanges at the level of the thermal solar collector

The mathematical models governing the different physical phenomena that occur at the level of the solar collector are the following:

Absorber 1 (inclined 20°)

$$e_{ab}\rho_{ab}Cp_{ab}\frac{dT_{ab1}}{dt} = \alpha_{ab}Ih_{Si,\alpha} + h_{r,ab1-vc}(T_{vc} - T_{ab1}) + h_{c,ab1-ae}(T_{ae} - T_{ab1}) + h_{r,ab1-pa}(T_{pa} - T_{ab1}) + h_{c,ab1-fc}(T_{fc} - T_{ab1}) \quad (1)$$

Absorber 2 (inclined 55°)

$$e_{ab}\rho_{ab}Cp_{ab}\frac{dT_{ab2}}{dt} = \alpha_{ab}Ih_{Si,\beta} + h_{r,ab2-vc}(T_{vc} - T_{ab2}) + h_{c,ab2-ae}(T_{ae} - T_{ab2}) + h_{r,ab2-pa}(T_{pa} - T_{ab2}) + h_{c,ab2-fc}(T_{fc} - T_{ab2}) \quad (2)$$

Aluminum plate

$$e_{pa}\rho_{pa}Cp_{pa}\frac{dT_{pa}}{dt} = h_{r,ab1-pa}(T_{ab1} - T_{pa}) + h_{c,pa-fc}(T_{fc} - T_{pa}) + h_{c,pa-ai}(T_{ai} - T_{pa}) \quad (3)$$

Coolant

$$\rho_{fc}v_{fc}Cp_{fc}\frac{dT_{fc}}{dt} = h_{c,ab1-fc} \times S_{ab1}(T_{ab1} - T_{fc}) + h_{c,pa-fc} \times S_{pa1}(T_{pa} - T_{fc}) + h_{c,ab2-fc} \times S_{ab2}(T_{ab2} - T_{fc}) + h_{c,pa-fc} \times S_{pa2}(T_{pa} - T_{fc}) \quad (4)$$

2.2.2. Modeling of the drying chamber

Figure 6 shows the heat exchanges at the level of the drying chamber.

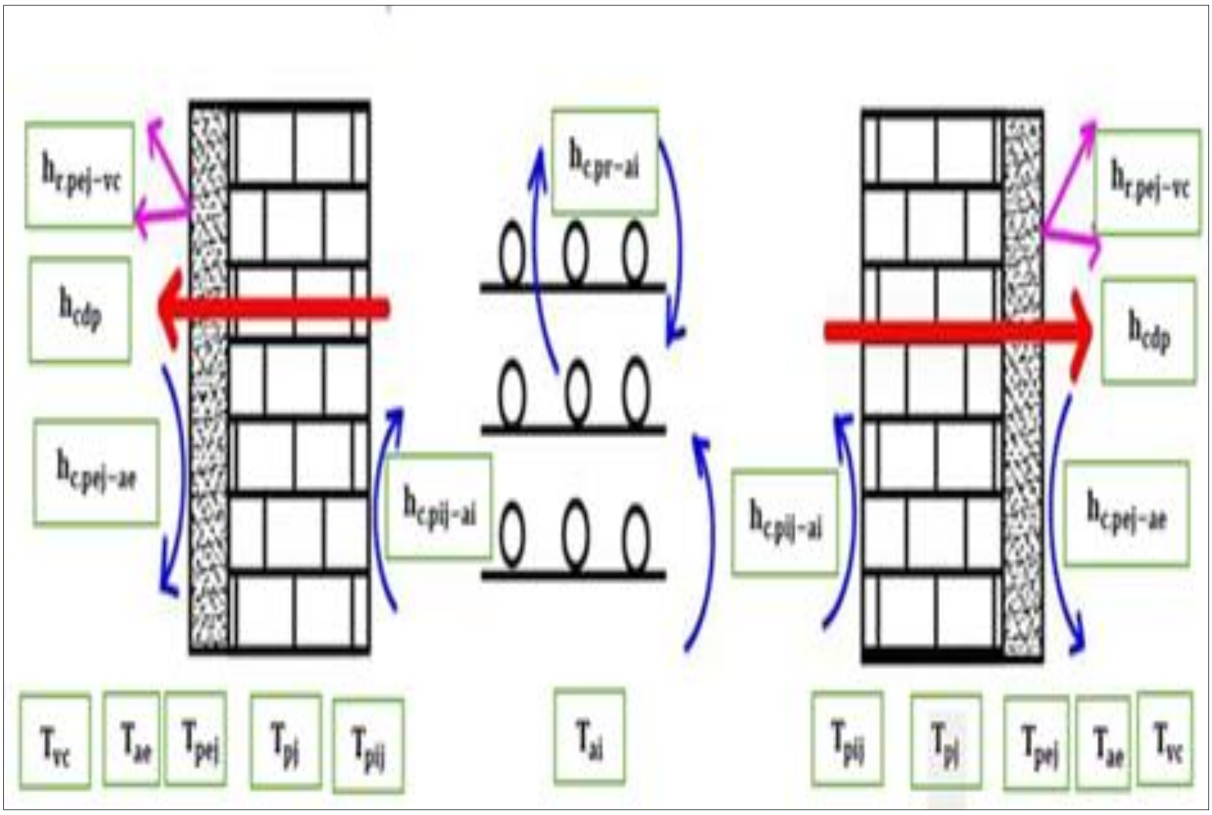

Figure 6 Schematic representation of heat exchanges in the drying chamber

The heat exchanges at the level of the drying chamber are modeled by the equations below:

Exterior and interior surface of vertical wall 1 (North-West)

$$e_p\rho_p Cp_p \frac{dT_{pe1}}{dt} = \alpha_p I h_{1,90} + h_{c,pe1-ae}(T_{ae} - T_{pe1}) + h_{r,pe1-vc}(T_{vc} - T_{pe1}) + hcdp \times (T_{p1} - T_{pe1}) \quad (5)$$

$$e_p\rho_p Cp_p \frac{dT_{pi1}}{dt} = h_{c,pi1-ai}(T_{ai} - T_{pi1}) + hcdp \times (T_{p1} - T_{pi1}) \quad (1)$$

Exterior and interior surface of vertical wall 2 (North-East)

$$e_p\rho_p Cp_p \frac{dT_{pe2}}{dt} = \alpha_p I h_{2,90} + h_{c,pe2-ae}(T_{ae} - T_{pe2}) + h_{r,pe2-vc}(T_{vc} - T_{pe2}) + hcdp \times (T_{p2} - T_{pe2}) \quad (7)$$

$$e_p\rho_p Cp_p \frac{dT_{pi2}}{dt} = h_{c,pi2-ai}(T_{ai} - T_{pi2}) + hcdp \times (T_{p2} - T_{pi2}) \quad (8)$$

Exterior and interior surfaces of vertical wall 3 (South-West)

$$e_p\rho_p Cp_p \frac{dT_{pe3}}{dt} = \alpha_p I h_{3,90} + h_{c,pe3-ae}(T_{ae} - T_{pe3}) + h_{r,pe3-vc}(T_{vc} - T_{pe3}) + hcdp \times (T_{p3} - T_{pe3}) \quad (9)$$

$$e_p\rho_p Cp_p \frac{dT_{pi3}}{dt} = h_{c,pi3-ai}(T_{ai} - T_{pi3}) + hcdp \times (T_{p3} - T_{pi3}) \quad (10)$$

Vertical wall 1

$$e_p \times \rho_p \times Cp_p \times \frac{dT_{p1}}{dt} + hcd_p \times (T_{p1} - T_{pe1}) = e_p \times \rho_p \times Cp_p \times \frac{dT_{p1}}{dt} + hcd_p \times (T_{p1} - T_{pi1}) \quad (11)$$

Vertical wall 2

$$e_p \times \rho_p \times Cp_p \times \frac{dT_{p2}}{dt} + hcd_p \times (T_{p2} - T_{pe2}) = e_p \times \rho_p \times Cp_p \times \frac{dT_{p2}}{dt} + hcd_p \times (T_{p2} - T_{pi2}) \quad (12)$$

Vertical wall 3

$$e_p \times \rho_p \times Cp_p \times \frac{dT_{p3}}{dt} + hcd_p \times (T_{p3} - T_{pe3}) = e_p \times \rho_p \times Cp_p \times \frac{dT_{p3}}{dt} + hcd_p \times (T_{p3} - T_{pi3}) \text{........... (13)}$$

Drying air (drying air)

$$\rho_{ai} \times V_c \times Cp_{ai} \frac{dT_{ai}}{dt} = h_{c,ai-pi1} \times S_{p1}(T_{pi1} - T_{ai}) + h_{c,ai-pi2} \times S_{p2}(T_{pi2} - T_{ai}) + h_{c,ai-pi3} \times S_{p3}(T_{pi3} - T_{ai}) + h_{c,pa-ai} \times S_{pa1}(T_{pa1} - T_{ai}) + h_{c,pa-ai} \times S_{pa2}(T_{pa2} - T_{ai}) + \rho_{fc} \times v_{fc} \times Cpai \times (T_{fc} - T_{ai}) \text{............. (14)}$$

About the product

$$m_p C_{pp} \frac{dT_{pr}}{dt} = h_{c,pr-ai} S_{pr}(T_{ai} - T_{pr}) - \dot{m} L_v \text{ ....(15)}$$

$$C_{pp} = C_{ps} + X.C_{pe} \text{ [11] .... (16)}$$

$$L_v = 4186,8 \times (597 - 0,56 T_{pr}) \text{ [11]......................(17)}$$

$\dot{m}$: rate of evaporation of water from the product ($kg_{eau}/kg_{ms}.s$)
L_v : latent heat of evaporation of water (J/kg)
S_p : exchange surface (m^2)
C_{pp} : mass heat capacity of the product ($J/kg.K$)
C_{ps} : specific heat capacity of water($J/kg.K$)
X : product water content (kg_{eau}/kg_{ms})

2.3. Mass balance

$$\dot{m} = -ms \times \frac{dX}{dt} \text{ .... (18)}$$

Based on Page's correlation [12],

$$\frac{dX}{dt} = (X_0 - X_e) \times (-k \times n \times t^{n-1}) \times exp(-kt^n) \text{...................... (19)}$$

With:

$$k = 0,048 - 0,003Tai + 0,016HR + 4,696 \times 10^{-5} Tai^2 - 0,03HR^2 \text{ .... (20)}$$

$$n = 1,521 + 0,046Tai - 3,432HR + 0,001Tai^2 + 3,293HR^2 \text{ ....(21)}$$

3. Results and discussion

3.1. Solar Radiation

The global solar irradiance on an inclined plane, received by our solar thermal collector, is extracted from the PVGIS database [13] (longitude = 10.30°, latitude = 1.38°, and altitude = 429 m) considering the 344th day of the year (December 10). Thus, for the different inclinations of the absorbers of the thermal solar collector, we obtain the irradiances below:

On the two absorbers-oriented South-East

Figure 7 shows the evolution of global solar irradiance received by absorber 1 inclined by 20° (Ihab1) and received by absorber 2 inclined by 55° (Ihab2).

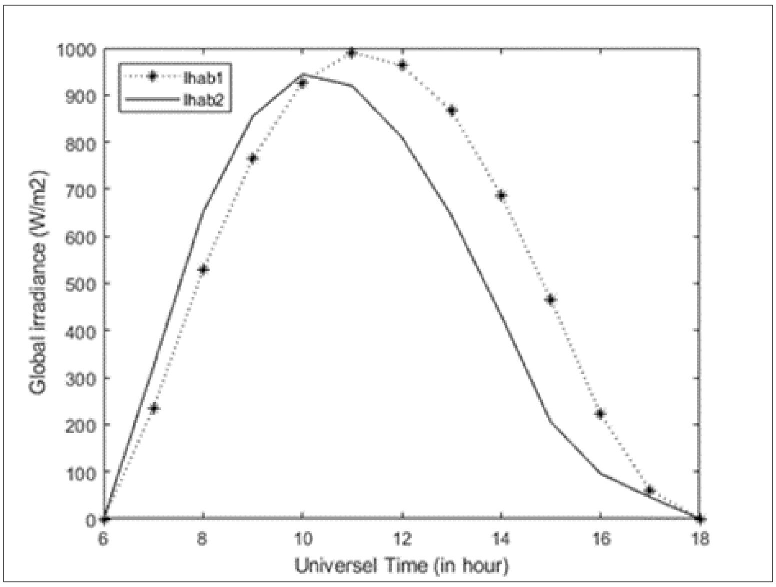

Figure 7 Global solar irradiance received by absorbers

We note that the global solar irradiance received by absorber 1 increases from sunrise to reach a maximum value of 990 W/m^2 around 12h TL (Local Time) corresponding to 11h UT (Universal Time) then then decreases to zero around 7 p.m. TL. On the other hand, the evolution of the global solar irradiance received by absorber 2 increases from sunrise to reach its maximum value of 944 W/m^2 around 11h TL this time then gradually decreases until to a zero value around 7 p.m. TL.

3.2. Evolution of the Temperature of the Heat transfer fluid, the Interior air and that of the product as a function of time

Figure 8 shows us the evolution of the temperature of the heat transfer fluid, the indoor air and the product.

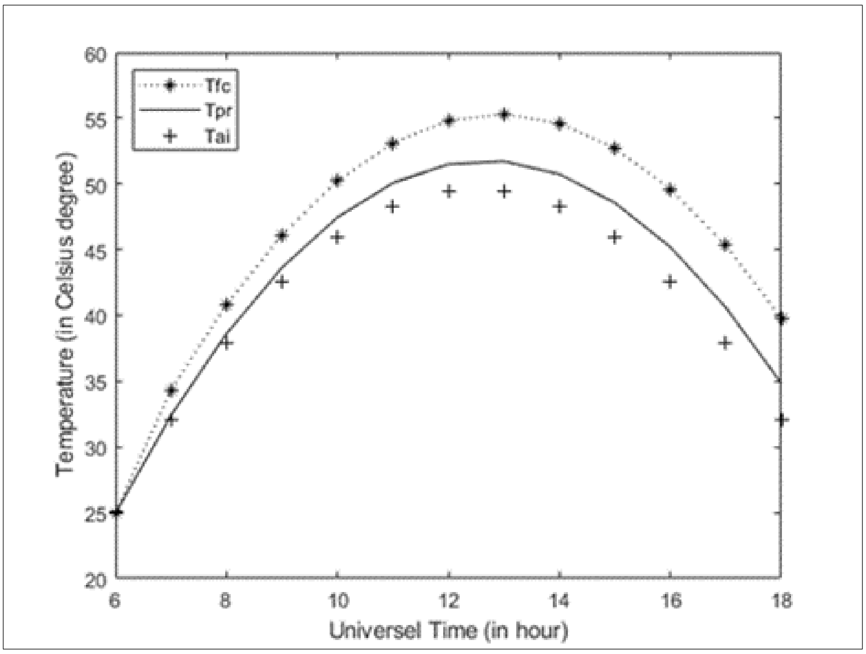

Figure 8 Evolution of the temperature of the heat transfert fluid, the indoor air and the product

At the level of the evolution of the temperature of the heat transfer fluid at the outlet of the solar collector, we can see that the temperature of the heat transfer fluid increases until it reaches a maximum value around 12h before starting to decrease. This shape results from the fact that the ambient air temperature is high in contact with the inner surface of the absorbers.

With regard to the indoor air temperature, we can see that the evolution of this temperature during the day follows almost the same pace as the evolution of the temperature of the heat transfer fluid, but the temperature of the heat transfer fluid always remains higher than the indoor air temperature. This difference is explained by the fact that the heat transfer fluid, once in the drying chamber, mixes with the air already in this chamber; thus, its temperature is lowered by a few degrees.

The curve reflecting the evolution of the temperature of the product (piece of cassava) shows us that at the start of drying, the pieces of cassava are almost at the same temperature as the indoor air. From 8 a.m., the temperature of the product begins to be higher than the temperature of the interior air.

3.3. Kinetics of drying

Figure 9 shows the evolution of the water content and Figure 10 shows the evolution of the drying rate of cassava pieces as a function of time. The analysis of these two curves clearly shows us the different classic phases of drying and indicates a drying time equal to 8 hours (from 7h to 15h TL).

Indeed, the appearance of these curves (figure 9 and figure 10) presents three phases, namely:

- A first phase of drying (increasing drying speed) at an almost constant rate between 7 am and 9 am TL which corresponds to the heating phase of the pieces of fresh cassava. We can see that this period is very short compared to the overall drying time.
- A second drying phase (constant drying rate) at a strongly decreasing rate corresponding to high moisture evaporation rates. During this period (from 8 a.m. to 12 p.m. TL approximately), we essentially note the evaporation of the free water found on the surface of the product and which is constantly renewed by the water coming from inside the product. This water migration is undoubtedly a factor limiting the rate of drying after this phase;
- A third phase of drying (slowing of the drying rate) corresponding to a somewhat slow evaporation period compared to the rate of evaporation during the previous phase. Indeed, the free water that was migrating from the interior to the exterior completely disappeared at the end of the previous phase. Only the bound water remains, which does not evaporate on the surface but inside the product. At this stage, the evaporation front is sinking towards the core of the product and the further this front is from the outer surface of the product, the more difficult water migration is. Hence the slower decrease observed between 12 p.m. and 3 p.m. TL before reaching the equilibrium water content of the product.

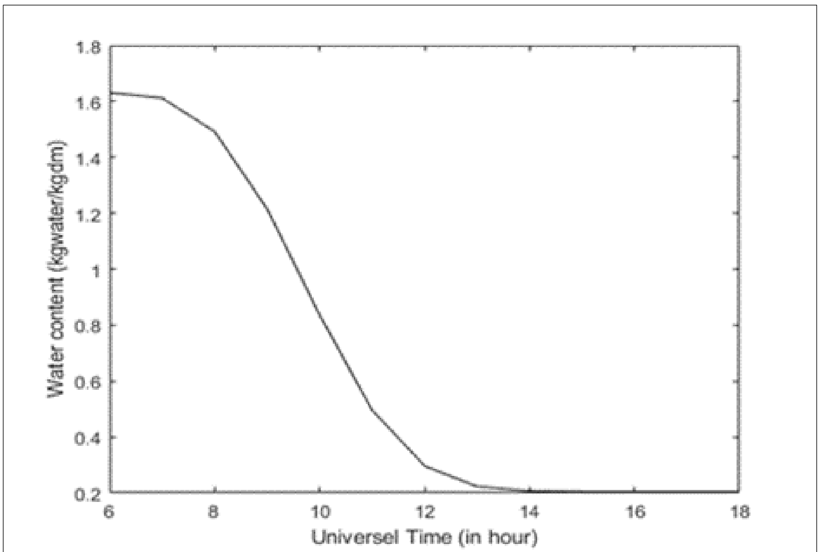

Figure 9 Evolution of the water content of cassava pieces

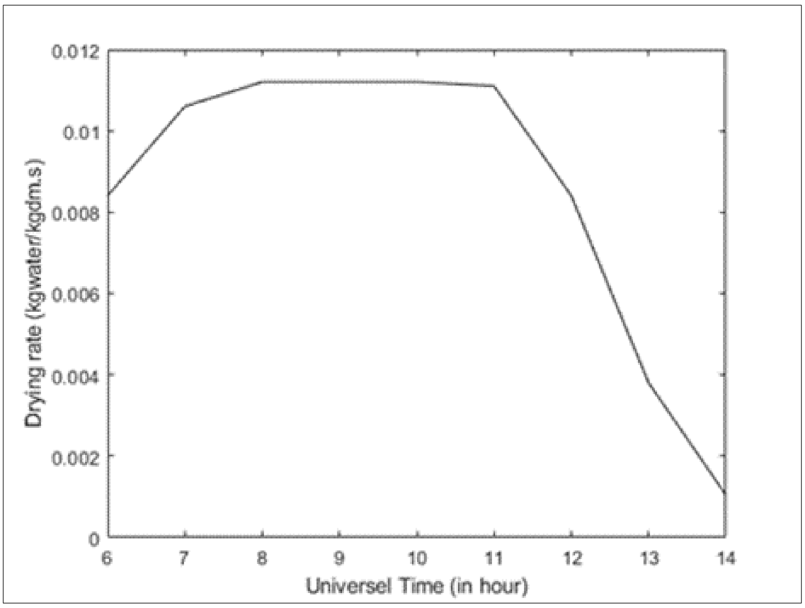

Figure 10 Evolution of the drying rate of cassava pieces

This drying kinetics of cassava pieces shows a similarity with that obtained experimentally by B. K. KOUA et al. [14]. But a difference appears between these two results at the start of drying. Indeed, with the theoretical model, the warming-up phase stands out, on the other hand with the experiment carried out by B. K. KOUA et al. [14], this first phase does not exist. This difference would be due not only to the better precision given by the Page model but also to the experimental approach used.

3.4. Dryer Performance

This part involves determining the hourly quantity of water evaporated from the cassava pieces by the dryer knowing that the quantity of cassava pieces to be dried is 501.4 kg for a drying time (ts) evaluated at 8 hours, with an initial water content of 162% for a final water content of 20% on a dry basis.

Let V_{ev} be the rate of evaporation of water by the dryer or the hourly quantity of water evaporated [11],

$V_{ev} = \frac{M_t}{t_s} \times \frac{x_{wi}-x_{wf}}{100-x_{wf}}$………………………. .(22)

x_{wi} : Initial water content on a wet basis of a piece of cassava;
x_{wf} : Final water content on a wet basis of a piece of cassava;
M_t : Total mass of piece of fresh cassava pieces (kg) ;
t_s : Drying time (h).

We obtain:

$$V_{ev} = \frac{501{,}4}{8} \times \frac{62-17}{100-17}$$

From where:

$$V_{ev} = 33{,}98 \text{ kgeau/h}$$

The main objective of this work was to model and simulate the operation of a prototype large-capacity indirect solar dryer for cassava drying. To achieve this objective, we first carried out a review of the bibliography on the raw material which is cassava and on the phenomenon of drying as well as the different technologies of solar dryers. This review of the bibliography has enabled us to observe that the technique of preservation by drying seems to be mastered, but in Benin mainly the drying of cassava is still artisanal, which does not guarantee a good quality of products from dried cassava chips. We then proceeded to choose the components of the indirect solar dryer prototype whose capacity is estimated at 501.4 kg of fresh cassava pieces at an initial water content of 163% on a dry basis, which corresponds to a mass of 208.15 kg of dry cassava pieces. As a result, we presented a model simulating the operation of this dryer. This model integrates the modeling of the thermal solar collector as well as the modeling of the drying chamber. A calculation program was developed in the MATLAB environment to globally simulate the operation of the indirect solar dryer prototype. Finally, the drying kinetics indicates a drying time of 8 hours (for a drying cycle starting at 7 a.m. Local Time) to bring the cassava pieces from their initial water content to the equilibrium water content.

The use of this dryer prototype will not only make it possible to take advantage of the available solar resource but to guarantee the nutritional value of the products derived from dried cassava pieces.

Abbreviations

Symbol	**Name**	**Unity**
S	Area	m^2
X	Water content on dry basis of cassava	kg_{water}/kg_{ms}
x_w	Water content on a wet basis of cassava	kg_{water}/kg_{ms}
T	Temperature	K
hr	Radiative exchange coefficient	$(W/m^2.K)$
hc	Convective heat transfer coefficient	$W/m^2.K$
hcd	Conductive exchange coefficient	$W/m^2.K$
$Ih_{Si,\alpha}$	Global solar irradiance received by absorber 1	W/m^2
$Ih_{Si,\beta}$	Global solar irradiance received by absorber 2	W/m^2
m	Product water evaporation rate or drying rate	$kg_{water}/kg_{ms}.s$
L_v	Latent heat of evaporation of water	J/kg
S_p	Exchange area	m^2
C_{pp}	Mass heat capacity of the product	$J/kg.K$
C_{ps}	Specific heat capacity of water	$J/kg.K$
V_{vent}	Average wind speed at the site	m/s
C_p	Mass heat capacity	$J.kg^{-1}. K^{-1}$
e_b	Brick thickness	M
e_{cr}	Plaster thickness	M
V_{a-pr}	Average speed of air flow over the product	m/s
τo	Filling rate of each drying rack	-
V_c	Volume of the drying chamber	m^3

Greek letters	**Names**	**Unity**
α	Tilt of absorber 1	o
β	Tilt of absorber 2	o
Indices	**Désignations**	
Ae	Outdoor ambient air	
Ai	Indoor air	

ab1	Absorber 1
ab2	Absorber 2
Vc	vault of heaven
Fc	Coolant
pej	Coolant
Pj	Vertical wall j
Pij	Inner surface of the vertical wall j
Pa	Aluminum plate

4. Conclusion

The main objective of this work was to model and simulate the operation of a prototype large-capacity indirect solar dryer for cassava drying. To achieve this objective, we first carried out a review of the bibliography on the raw material which is cassava and on the phenomenon of drying as well as the different technologies of solar dryers. This review of the bibliography has enabled us to observe that the technique of preservation by drying seems to be mastered, but in Benin mainly the drying of cassava is still artisanal, which does not guarantee a good quality of products from dried cassava chips. We then proceeded to choose the components of the indirect solar dryer prototype whose capacity is estimated at 501.4 kg of fresh cassava pieces at an initial water content of 163% on a dry basis, which corresponds to a mass of 208.15 kg of dry cassava pieces. As a result, we presented a model simulating the operation of this dryer. This model integrates the modeling of the thermal solar collector as well as the modeling of the drying chamber. A calculation program was developed in the MATLAB environment to globally simulate the operation of the indirect solar dryer prototype. Finally, the drying kinetics indicates a drying time of 8 hours (for a drying cycle starting at 7 a.m. Local Time) to bring the cassava pieces from their initial water content to the equilibrium water content.

The use of this dryer prototype will not only make it possible to take advantage of the available solar resource but to guarantee the nutritional value of the products derived from dried cassava pieces.

Future scope

It is planned to simulate the functioning of this prototype taking into account meteorological data from other areas of Benin which also produce a large quantity of cassava; then test with the proposed model, other agri-food products in order to establish a list of consumer products that can be dried by this dryer apart from cassava.

Compliance with ethical standards

Acknowledgments

Thanks go to all those who have financially supported this project and also those who share their comments have improved the quality of this work.

Disclosure of conflict of interest

It is declared that there are no conflicting interests among all three authors.

References

[1] O. BEUCHER et al, (November 2012) " Agriculture in Africa facing the challenges of climate change ", Institute of Energy and Environment of La Francophonie, p.170.

[2] D. Acclassato, "Ten Yen After the Maputo Declaration on and Agriculture and Food Security: An Assessment of Progress in West Africa Structure and content of country studies", p.32.

[3] A. D. MBALLO, (2018) "Post-harvest loss measurements in Africa ", Food and Agriculture Organization of the United Nations, p.9.

[4] C. AHOUANNOU (2001), "Study of the drying of tropical food products, application to cassava, ginger, okra and pepper", Doctoral thesis, National University of Benin.

[5] S. Khaldi, "Numerical study of the thermal behavior of a solar dryer using a thermal bed for energy storage", p. 141.

[6] A. Ferradji, Y. Goudjal and A. Malek, (2008) "Drying of sultana variety grapes by a forced convection solar dryer and a shell type dryer", p.9.

[7] A. BOUSSALIA (2010) «Contribution to the study of solar drying of local agricultural products ". » magister dissertation, MENTOURI-CONSTANTINE University (Algeria), p.119.

[8] R. Dilip Pangavhane, R. I. Sawhney, P. N. Sarsavadia, (2002) « Design, development and performance testing of new natural convection solar dryeer », 2002, 579-590.

[9] Jain, (2007) « Modeling the performance of the reversed absorber with packed bed thermal storage natural convection solar crop dryer », J. Food Eng., vol. 78, no 2, p. 637-647.

[10] S. Singh, Parm Pal Singh, S. Dhaliwal, (2004) « multi-shelf portable solar dryer », Renewable energy, 753-765.

[11] O. Hospice BOLADJI (2010) «Improvement of shea kernel drying in central and northern Benin: Participatory design and sizing of an indirect solar dryer with greenhouse effect», Final dissertation for obtaining the Design Engineering Diploma, University of Abomey-Calavi, p.117.

[12] C. He et al., (2021, March) « Drying Behavior and Kinetics of Drying Process of Plant-Based Enteric Hard Capsules », Pharmaceutics, vol. 13, no 3, p. 335, doi: 10.3390/pharmaceutics13030335.

[13] JRC Photovoltaic Geographical Information System (PVGIS) - European Commission ». https://re.jrc.ec.europa.eu/pvg_tools/en/tools.html (accessed 1 October 2021).

[14] B. Koua, W. Fassinou, P. Gbaha, et S. Toure, (2007) « Experimental study of cassava drying kinetics in a direct solar dryer equipped with a thermal circulator », Rev Ivoir Sci Technol, vol. 9, p. 11-26, janv.